Soft Matter

ROYAL SOCIETY
OF CHEMISTRY

PAPER
Dong Ki Yoon *et al.*
Creation of liquid-crystal periodic zigzags by surface treatment and
thermal annealing

PAPER

Creation of liquid-crystal periodic zigzags by surface treatment and thermal annealing†

Seong Ho Ryu,[a] Min-Jun Gim,[a] Yun Jeong Cha,[a] Tae Joo Shin,[b] Hyungju Ahn[c] and Dong Ki Yoon*[a]

The orientation control of soft matter to create a large area single domain is one of the most exciting research topics in materials science. Recently, this effort has been extended to fabricate two- or three-dimensional structures for electro-optical applications. Here, we create periodic zigzag structures in liquid crystals (LCs) using a combination of surface treatment and thermal annealing. The LC molecules in the nematic (N) phase were initially guided by the alignment layer of rubbed polymers, which were quenched and subsequently annealed in the smectic A (SmA) phase to create periodic zigzag structures that represent modulated layer structures. Direct investigation of the zigzags was performed using microscopy and diffraction techniques, showing the alternately arranged focal conic domains (FCDs) formed. The resulting macroscopic periodic structures will be of interest in further studies of the physical properties of soft matters.

Introduction

Self-assembly of soft matters such as surfactants, lipids, block copolymers, and liquid crystals (LC), has been of interest because of the convenience to manipulate the various kinds of micro- and nano-structures.[1–3] Especially, the fabrication of a large area single domain of soft matters without defects is the key issue in material sciences and nanotechnologies.[4–8] Numerous methods have been introduced to achieve this goal, including surface treatment, topographic confinement, and the application of electric or magnetic fields.[9–13] Among these, surface treatment is the easiest and cheapest approach to obtain desirable structures and has been the most widely used technique even in industry.[14,15] For example, homeotropic or planar alignment of LC molecules can be achieved on molecule-phobic or -philic substrates.[16–18]

In particular, the orientation control of the smectic A (SmA) phase, that has layered structures composed of one-dimensionally (1D) aligned molecules, has been intensively studied because of its unique optical and topographical morphologies.[19,20] One of the interesting textures of the SmA phase is the focal conic domain (FCD), in which layers are wrapped around the conjugated ellipse and hyperbola defect lines, leading to layer bending toward the defect line because of the balance between the bulk elasticity and boundary conditions.[21–23] This micron-scale structure can be self-organized into well-ordered arrays with neighbouring FCDs,[24,25] enabling the use of smectic LCs in lithographic applications such as soft lithography,[6] microlens arrays,[26] superhydrophobic surfaces,[27] and trapping tools of particles.[20,28] In addition, many attempts have been made to shape FCDs in the SmA LC phase. For example, linearly arranged toric FCDs (TFCDs) were obtained in the micro-confined geometry,[20] and the rectangular or flower-like organization of FCDs has been reported.[29–32] Most recently, sublimable LC materials formed three-dimensional dome-like structures with concentric rings at the nanometer scale.[33,34]

Here, the periodic zigzag patterns were generated on the rubbed polyimide (PI)-alignment layer using two-step thermal treatments: quenching and annealing. And a key clue to understand the origin of the zigzag structure was found during the phase transition between the SmA and the nematic (N) phase, in which the translational symmetry of smectic layers along the rubbed direction was spontaneously broken in the form of periodic FCDs. Depolarized reflection light microscopy (DRLM), laser-scanning fluorescent confocal microscopy (LSFCM), and atomic force microscopy (AFM) were used to investigate the molecular orientation and layer structures in the zigzag structures. Quantitative analysis of the zigzag structure was also performed using the grazing incident X-ray diffraction (GIXD) technique.

Results and discussion

Formation of zigzag structures and their optical observation

One of the most common LC materials, 8CB (4′-*n*-octyl-4-cyano-biphenyl), was melt at the isotropic temperature and dropped-spin coated on the rubbed PI-coated silicon (Si) substrate at

a Graduate School of Nanoscience and Technology and KINC, KAIST, Daejeon, 305-701, Republic of Korea. E-mail: nandk@kaist.ac.kr; Tel: 82-42-350-1156
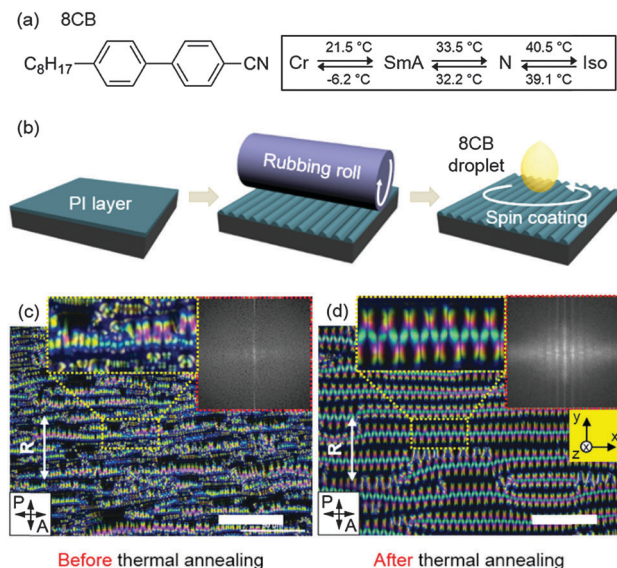*b UNIST Central Research Facilities & School of Natural Science, UNIST, Ulsan, 689-789, Republic of Korea*
c Pohang Accelerator Laboratory, POSTECH, Pohang, 790-784, Republic of Korea
† Electronic supplementary information (ESI) available: See DOI: 10.1039/c5sm01989c

Fig. 1 Sample information, experimental procedures, and DRLM images of the zigzag structures. (a) The molecular structure of 8CB and its thermal phase transition temperatures. (b) Schematic illustration of experimental procedures. (c) The broken FCDs and irregular zigzag structures are appeared in the thermally quenched sample, while (d) the well-ordered zigzag structures are formed after the thermal annealing. R corresponds to the rubbing direction. Yellow and red boxes show the enlarged optical textures of the zigzags in a line and the fast Fourier transform (FFT) images, respectively. The scale bars are 50 μm.

room temperature which corresponds to the SmA phase (Fig. 1a and b). During this simple process, the thermal quenching of the LC sample occurs from the isotropic to SmA phase, and the spin coating process makes the LC film uniformly thin on the substrate. This film was then thermally annealed at just below the SmA–N transition temperature at 33.4 °C for a few minutes until the LC molecules were re-aligned along the rubbed direction, R. The resultant LC textures were examined by DRLM. The as-spin-coated sample has the non-uniformly generated zigzag structures (Fig. 1c) which are merged with neighbouring broken domains to form well-ordered zigzags after the thermal annealing process in the entire sample area, ∼several mm^2 (Fig. 1d), and the size of the zigzag structure is proportional to the sample thickness (Fig. S1 in the ESI†).

During cooling from the isotropic state, 8CB molecules intrinsically show both N and SmA phases, and the molecular director of LC molecules, n, is aligned along R at the N phase, remaining at the initial orientation near the substrate even after the phase transition to the SmA phase. As a result of the thermal annealing process, n is globally frustrated relative to R, i.e., the zigzags are indicative of the periodic modulation of n and the side-by-side arranged LC molecules in the SmA phase.[35] This phenomenon can be confirmed by the high intensity revealed within 20°-rotated crossed polarizers and the complete extinction at 45° rotation (Fig. S2 in the ESI†). The fast Fourier transform (FFT) images reveal completely different results in terms of the structural regularity before and after the thermal annealing process, in which the quenched sample shows no notable peaks (the red box in Fig. 1c), while the annealed sample exhibits clear dot

patterns, indicating the regularly ordered morphologies (the red box in Fig. 1d).

To see the exact in-plane and out-of-plane molecular orientation of the zigzags, LSFCM experiments with a linearly polarized laser source were performed. And 0.01 wt% of n,n -bis(2,5-di-tert-butylphenyl)-3,4,9,10-perylenedicarboximide (BTBP) fluorescent dye molecules were mixed with 8CB to reveal the molecular orientation.[36] The fluorescence intensity in the LSFCM image was measured as a function of angle α between n and the excited polarization direction of laser, Pol, i.e., the intensity is maximized when Pol is parallel with n. In-plane molecular orientation at a certain z-axis position, z = 4 μm, was investigated and the cross-sectional views revealed the out-of-plane textures of the zigzags. The total thickness of 8CB was estimated to be ∼7 μm by the extinction of the fluorescent intensity measured along the z-direction (Fig. S3 in the ESI†).

As shown in Fig. 2a, the fluorescence intensity of the xy plane view at z = 4 μm was varied as a function of α, where bright elliptic morphologies were observed at α ∼ 0°, while these were vanished at α ∼ 90° (Fig. 2b). For 0 μm ≤ z ≤ 7 μm of the sample, the cross-section views of Fig. 2a and b on the yz plane were obtained at three points indicated by i, ii, and iii along the x-axis (Fig. 2c). As reported previously, the FCD consists of a hyperbola in the cross-sectional image because of the tangentially aligned layers.[25,37] When Pol is parallel to the y-axis, two bright hyperbolas appear, where the smaller hyperbola at i gradually grows as the scan direction moves toward iii and vice versa because the LC molecules are modulated along this direction, as expected in the DRLM images (Fig. 1d). This behaviour results from the change of n with splay deformation induced by the contribution of surface anchoring and bulk elasticity, in which the layers bend in the interconnecting areas
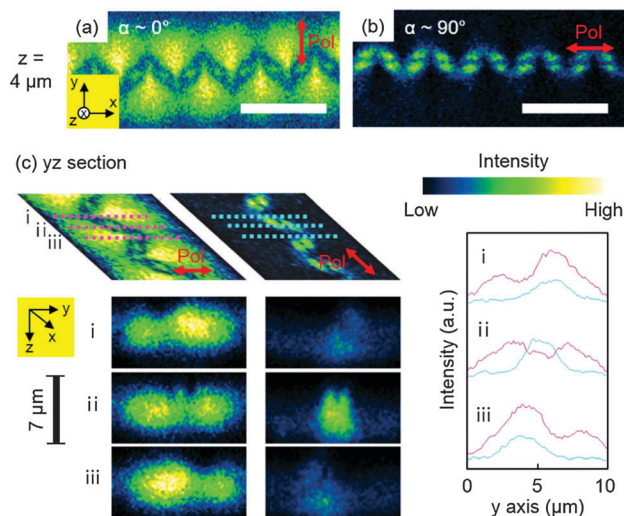

Fig. 2 LSFCM images of the zigzag structures in a line depending on the direction of the excited polarized laser (Pol). The xy plane images obtained at z = 4 μm (a) under the parallel Pol to the y-axis, (b) under perpendicular Pol to the y-axis. (c) Cross-sectional LSFCM images at the certain positions are indicated by the magenta and cyan colour lines and the relative intensity profiles. The scale bars are 10 μm.

between FCDs, as evidenced by the periodic dark and bright regions along the *x*-axis in Fig. 2a and c, respectively. The overall fluorescent intensity clearly reveals that most of the LC molecules are aligned parallel to the *y*-axis, *R*. In addition, the weak fluorescent intensity near the LC/air boundary as well as the bottom substrate indicates that the LC molecules are homeotropically aligned.

GIXD and AFM studies to determine the molecular and layer orientation of the zigzags

The molecular level arrangement of the smectic layering structures in the zigzags was examined by GIXD experiments employing a synchrotron source at the 9A beamline of the Pohang accelerator laboratory (PAL) at room temperature, which corresponds to the SmA phase. The small incidence angle ($\theta \sim 0.1°$) of the X-ray beam (B) was used to directly determine the in-plane as well as out-of-plane information of the layer and molecular arrangement of the zigzags with a two-dimensional charge coupled device (CCD) camera, as described in Fig. 3a.
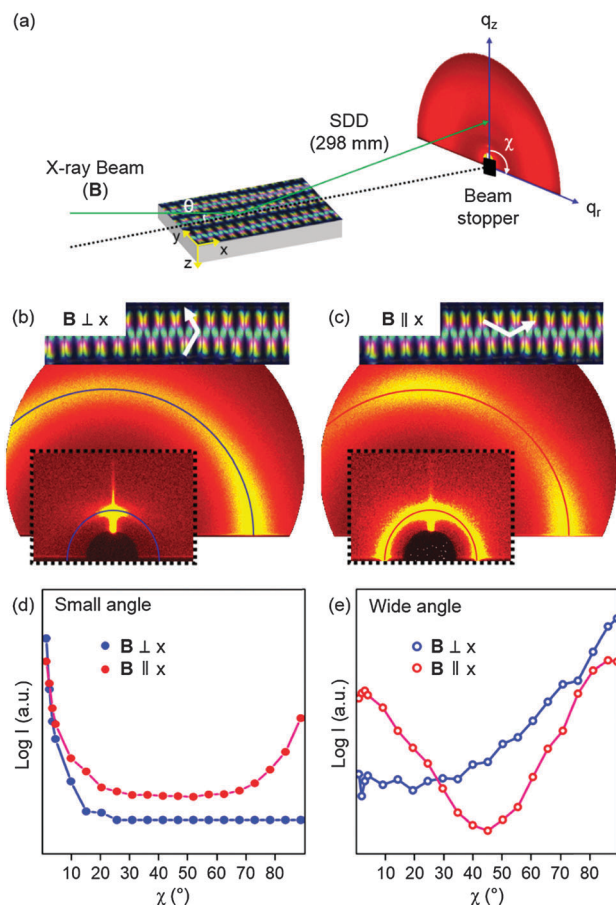

Fig. 3 Experimental set-up of grazing incidence X-ray diffraction (GIXD) experiments, the resultant 2D GIXD patterns, and their 1D circular plots depending on the direction of the incident X-ray beam, B. (a) The incidence angle (θ) is $\sim 0.1°$ and χ is the azimuthal angle from q_z. The 2D GIXD patterns of the zigzag structures are obtained in different incident beam directions for (b) the B⊥*x*-axis and (c) the B∥*x*-axis. The peak intensities are analysed (d) in the small-angle region and (e) in the wide-angle region as a function of χ.

When B was perpendicular to the *x*-axis (or parallel to the *y*-axis), a very strong centre peak at $\chi \sim 0°$ was observed in the small-angle region, and a corresponding diffused peak was observed in the wide-angle regions at $\chi \sim 90°$ (Fig. 3b), indicating that most of the layer structures are located on the *xy* plane in the zigzag structure, as expected from the LSFCM observation. In contrast, when B is passed along the *x*-axis, ring patterns are observed in the small-angle region; however, the centre and side peaks at $\chi \sim 0°$, $90°$, and $-90°$ are especially strong, and the strongest peak at $\chi \sim 0°$ indicates that most of the smectic layers are still aligned parallel to the bottom substrate even though there are vertically aligned layers in this direction (Fig. 3c). This layer orientation was confirmed by the orthogonally oriented diffraction patterns in the wide-angle region.

The orientation of the layer structures in the zigzags can be quantitatively analysed in the azimuthally plotted one-dimensional graph, in which the peak intensities were plotted as a function of χ in the small- and wide-angle regions for the B⊥*x*-axis (blue) and the B∥*x*-axis (red) (Fig. 3d and e), in which the surface reflection effect is considered. The highest intensity in the small-angle region was found at $\chi \sim 0°$ in both cases, indicating that the layer structures with $q \sim 0.20$ nm^{-1} corresponding to 3.1 nm are aligned parallel with the *xy* plane and the bottom substrate as well (Fig. 3d). The strong wide-angle peaks at $\chi \sim 90°$ can explain the homeotropic aligned LC molecules at the LC/air interface and near the bottom substrate (Fig. 3e).[37] By the way, the small-angle peaks through $0 < \chi < 90°$ were also observed when B was parallel to the *x*-axis, indicating the tangentially aligned smectic layer structures on the *xy* plane to this direction.[20]

To obtain the topographic structure of the zigzags, AFM measurements were performed. For this, the tapping mode was used. As observed in the optical images (Fig. 1 and 2), the AFM image shows the modulated topography along the *x*-axis, alternately shifting high and low profiles along the *y*-axis, representing the periodic array of FCDs (Fig. 4a and Fig. S4, ESI†). The height profile of the AFM image (the inset of Fig. 4a) shows the
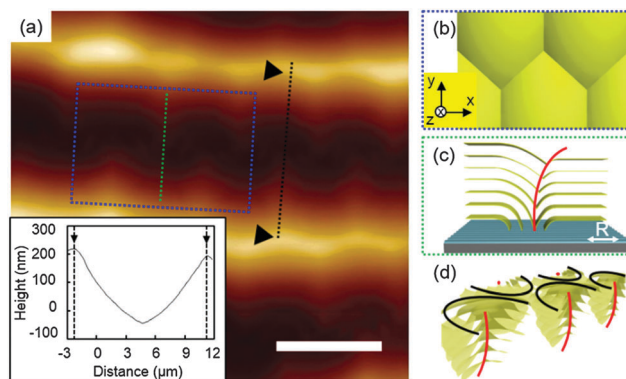
Fig. 4 AFM study and schematic illustrations of the layers in the zigzag structures. (a) The AFM topographic image of the zigzag structures and the inset show the height profile along the *y*-axis. The scale bar is 10 μm. (b) Top view model of the zigzags on the *xy* plane and (c) cross-section views on the *yz* plane and (d) perspective view with the ellipse and the hyperbola line indicated by the black and red lines, respectively.

surface topography of the zigzags along the y-axis, in which the maximum height difference is approximately 300 nm, which is very small considering that the thickness of the LC film is ∼7 μm. This can be explained by the competition among the surface tension, compressional elastic constant, and film thickness, as observed in FCD arrays confined in microchannels.[10,20]

The typical topographic structure boxed in Fig. 4a and Fig. S4 (ESI†) is illustrated in Fig. 4b–d, in which the FCDs are alternatively arranged through the x-axis, representing the intersected FCDs by disclination lines. Thus, in the layers near the top of the zigzags as well as the bottom substrate, n is perpendicular to these boundaries, as described in the cross-section and perspective views in Fig. 4c and d. This arrangement of FCDs completely agrees with the GIXD results, in which only planar smectic layers are observed on the substrate when B is parallel to R, whereas tangentially aligned layering structures are found when B is perpendicular to R (Fig. 3b–e).

The AFM imaging of the periodic height modulations is also supported by the DRLM images (Fig. S2, ESI†). Rotating cross-polarizers reveal changes in the birefringent colours of the zigzags, in which the colour changes from sky blue to pink and yellow along the y-axis in one FCD (the white box in Fig. S2, ESI†) because of the different LC molecular orientation in the splay deformation. The alternately packed FCDs produce periodic intensity changes from dark to bright along the x-axis. For example, the dark brush (the white arrow in Fig. S2a, ESI†) becomes the sky blue colour domain, indicating modulated n along the x-axis.

Growing sequences of the zigzags

In Fig. 5, the heating and subsequent cooling trace between the SmA and N phases reveals the structural transition of the zigzag

Fig. 5 Structural transition behaviour of the zigzag structure upon heating to the N phase and subsequent cooling to the SmA phase. (a and b) The transition of the zigzag structures to disclination lines occurs upon heating to the SmA–N phase transition temperature. (c) The texture becomes dark in the N phase (the inset shows the 45° rotated sample to show the well-aligned N phase). (d) 2D close-packed tilted FCDs appear in the SmA phase instead of the zigzag structures upon cooling from the N phase. The scale bars are 10 μm.

structures, which is compared with the tilted FCDs prepared on simply cooling from the isotropic phase.[25] Upon heating the sample to the SmA–N phase transition temperature (∼33.5 °C), the zigzag structures slowly disappeared with the disclination line, while the other parts became dark (Fig. 5a and b). The energy cost was relaxed by replacing the strong splay deformation of the zigzag structures in the SmA phase with the twist deformation near the SmA–N phase transition, resulting in the disclination lines,[38] which finally disappeared in the N phase (Fig. 5c). At this stage, the sample under 45°-rotated cross-polarizers exhibited the brightest intensity, meaning well-aligned LC molecules along R (the inset of Fig. 5c). With this sample, re-cooling from the N to SmA phase spontaneously generated 2D close-packed tilted FCD lattices (Fig. 5d).[25] The zigzags can reappear if the disclination lines do not disappear, indicating that most of the LC molecules in our system forget their positions once the temperature is elevated to the complete N-phase temperature although the sample is prepared on the rubbed substrate (Fig. S5 in the ESI†).
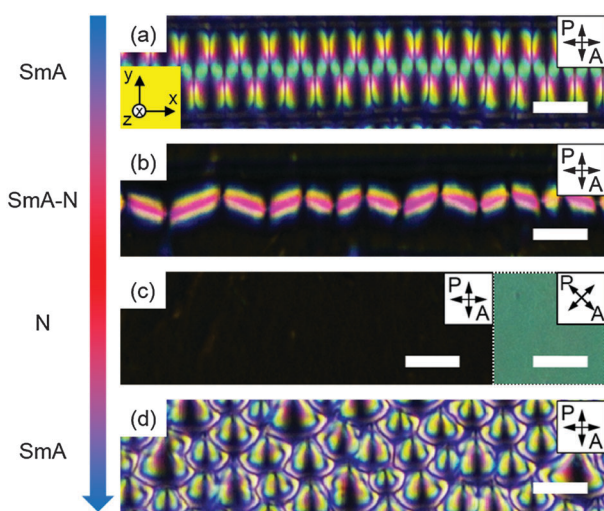
Based on this growing sequence experiment, the organization of the zigzags made at the SmA phase can be determined by two processes: first, quenching LC molecules on the rubbed polymer and second, subsequent slow cooling allows the LC molecules to have sufficient time to form regular-sized FCDs, which communicate each other through the layer propagation direction, x-axis, as demonstrated in Fig. 1, 4 and 5. This can explain how important the thermal annealing process is in the formation of the LC structures. The regular zigzag patterns can be explained by the free energy density estimation with Frank elastic constants (K_1) and layer compressibility modulus (B) as defined below.

$$F = \frac{1}{2}K_1(\mathrm{div}\,\mathrm{n})^2 + \frac{1}{2}B\left(\frac{d-d_0}{d_0}\right),$$

where d_0 is the equilibrium repeat distance, d is the actual layer thickness measured. As approaching to SmA–N transition temperature on heating, the B value becomes negligible, while K_1 does not significantly dependent on the temperature variation, therefore the total free energy decreases. The decrease of B induces the relaxed layers,[39] leading to the bigger FCDs, which is in the lower energetic state. This can be confirmed by comparing the quenched SmA texture and annealed SmA one and thus the density of the defect is decreased as compared with Fig. 1(c) and (d). Our simple but very effective thermal treatment can address FCDs that can grow into the zigzag structures in a large area of the order of several mm², which has not been achieved in the SmA system on flat substrates to date.

Conclusion

We created the periodic zigzag structures on rubbed PI-coated substrates using thermal quenching and annealing methods. LC molecules in the zigzags are mostly aligned parallel to the rubbing direction during phase transition from the N to SmA phase, but the alternatively packed FCDs were generated at the SmA phase though the perpendicular direction of n. This behaviour results from the splay deformation generated to balance the

surface anchoring effect and bulk elasticity of the smectic layers. Our resultant platform suggested in this work can enable us to make the large area organization of FCDs on the flat substrate and make LC morphologies rich to open up new challenges to study the unique structures of the other soft matters.

Experimental

Sample preparation

Si substrates were chemically cleaned using ultrasonication in acetone, followed by rinsing several times with ethanol and deionized water before being treated with O_2 plasma to remove any organic residue for 5 min. Planar anchoring was obtained by a spin-coating PI material on the Si substrate. The coated PI layer was soft-baked at 90 °C for 90 s and then hard-baked at 200 °C for 2 h before being mechanically rubbed using rubbing roll to yield a unidirectional orientation of the LC molecules (Fig. S6, ESI†). The LC sample, 4′-octyl-4-biphenylcarbonitrile (8CB), was coated on this rubbed PI-coated Si substrate using the spin-coating technique at the isotropic phase temperature and then annealed at 33.4 °C in the heating cycle using a heating stage (Linkam LTS 420 and TMS94). For the fluorescent imaging, 8CB was doped with 0.01 wt% of a fluorescent dye molecule, N,N'-bis(2,5-di-tert-butylphenyl)-3,4,9,10-perylenedicarboximide (BTBP), that is excited at 488 nm and emitted in the range of 510–550 nm.

Characterization

The birefringent textures of the LC sample were observed by DRLM (NIKON, LV100POL). The LSFCM measurements were carried out with a linearly polarized laser at a wavelength ∼488 nm (Nikon, C2 Plus). The topographical morphologies of the zigzag structures and the height profiles were examined using AFM (Bruker, Multimode-8) in the tapping mode with a high amplitude to prevent the tip contamination from the sticky LC sample. GIXD experiments were conducted at the 9A beam line of the Pohang accelerator laboratory (PAL). The size of the focused beam was ∼30 (V) × 290 (H) μm^2, and the energy was 11 keV. The sample-to-detector distance was fixed at 298 mm to investigate both the small-angle and wide-angle regions of the diffraction patterns. The GIXD results were collected using a 2D CCD detector (Rayonix SX165, USA).

Acknowledgements

Notes and references

1 H. A. Klok and S. Lecommandoux, *Adv. Mater.*, 2001, **13**, 1217.
2 T. Kato, *Science*, 2002, **295**, 2414.
3 G. M. Whitesides and B. Grzybowski, *Science*, 2002, **295**, 2418.
4 R. A. Segalman, H. Yokoyama and E. J. Kramer, *Adv. Mater.*, 2001, **13**, 1152.
5 R. Ruiz, H. Kang, F. A. Detcheverry, E. Dobisz, D. S. Kercher, T. R. Albrecht, J. J. de Pablo and P. F. Nealey, *Science*, 2008, **321**, 936.
6 H.-S. Moon, D. O. Shin, B. H. Kim, H. M. Jin, S. Lee, M. G. Lee and S. O. Kim, *J. Mater. Chem.*, 2012, **22**, 6307.
7 H.-W. Yoo, Y. H. Kim, J. M. Ok, H. S. Jeong, J. H. Kim, B. S. Son and H.-T. Jung, *J. Mater. Chem. C*, 2013, **1**, 1434.
8 M. Park, C. Harrison, P. M. Chaikin, R. A. Register and D. H. Adamson, *Science*, 1997, **276**, 1401.
9 X. Zhuang, L. Marrucci and Y. R. Shen, *Phys. Rev. Lett.*, 1994, **73**, 1513.
10 M. C. Choi, T. Pfohl, Z. Y. Wen, Y. L. Li, M. W. Kim, J. N. Israelachvili and C. R. Safinya, *Proc. Natl. Acad. Sci. U. S. A.*, 2004, **101**, 17340.
11 W. Guo, S. Herminghaus and C. Bahr, *Langmuir*, 2008, **24**, 8174.
12 F. Brochard, P. Pieranski and E. Guyon, *Phys. Rev. Lett.*, 1972, **28**, 1681.
13 I. Gryn, E. Lacaze, R. Bartolino and B. Zappone, *Adv. Funct. Mater.*, 2015, **25**, 142.
14 P. J. Shannon, W. M. Gibbons and S. T. Sun, *Nature*, 1994, **368**, 532.
15 M. Schadt, H. Seiberle and A. Schuster, *Nature*, 1996, **381**, 212.
16 S. Shojaei-Zadeh and S. L. Anna, *Langmuir*, 2006, **22**, 9986.
17 Y. H. Kim, D. K. Yoon, H. S. Jeong, O. D. Lavrentovich and H.-T. Jung, *Adv. Funct. Mater.*, 2011, **21**, 610.
18 S. D. Evans, H. Allinson, N. Boden, T. M. Flynn and J. R. Henderson, *J. Phys. Chem. B*, 1997, **101**, 2143.
19 K. Peddireddy, V. S. R. Jampani, S. Thutupalli, S. Herminghaus, C. Bahr and I. Musevic, *Opt. Express*, 2013, **21**, 30233.
20 D. K. Yoon, M. C. Choi, Y. H. Kim, M. W. Kim, O. D. Lavrentovich and H.-T. Jung, *Nat. Mater.*, 2007, **6**, 866.
21 P. G. de Gennes and J. Prost, *The Physics of Liquid Crystals*, Clarendon Press, Oxford, 1993.
22 J. B. Fournier, *Phys. Rev. Lett.*, 1993, **70**, 1445.
23 M. Kleman and O. D. Lavrentovich, *Liq. Cryst.*, 2009, **36**, 1085.
24 B. Zappone and E. Lacaze, *Phys. Rev. E: Stat., Nonlinear, Soft Matter Phys.*, 2008, **78**, 061704.
25 B. Zappone, C. Meyer, L. Bruno and E. Lacaze, *Soft Matter*, 2012, **8**, 4318.
26 Y. H. Kim, H. S. Jeong, J. H. Kim, E. K. Yoon, D. K. Yoon and H.-T. Jung, *J. Mater. Chem.*, 2010, **20**, 6557.
27 Y. H. Kim, D. K. Yoon, H. S. Jeong, J. H. Kim, E. K. Yoon and H.-T. Jung, *Adv. Funct. Mater.*, 2009, **19**, 3008.
28 D. S. Kim, A. Honglawan, K. Kim, M. H. Kim, S. Jeong, S. Yang and D. K. Yoon, *J. Mater. Chem. C*, 2015, **3**, 4598.
29 A. Honglawan, D. A. Beller, M. Cavallaro, R. D. Kamien, K. J. Stebe and S. Yang, *Adv. Mater.*, 2011, **23**, 5519.
30 A. Honglawan, D. A. Beller, M. Cavallaro, Jr., R. D. Kamien, K. J. Stebe and S. Yang, *Proc. Natl. Acad. Sci. U. S. A.*, 2013, **110**, 34.
31 D. A. Beller, M. A. Gharbi, A. Honglawan, K. J. Stebe, S. Yang and R. D. Kamien, *Phys. Rev. X*, 2013, **3**, 041026.

32 J. M. Ok, Y. H. Kim, H. S. Jeong, H.-W. Yoo, J. H. Kim, M. Srinivasarao and H.-T. Jung, *Soft Matter*, 2013, **9**, 10135.

33 D. K. Yoon, Y. H. Kim, D. S. Kim, S. D. Oh, I. I. Smalyukh, N. A. Clark and H.-T. Jung, *Proc. Natl. Acad. Sci. U. S. A.*, 2013, **110**, 19263.

34 D. S. Kim, Y. J. Cha, H. Kim, M. H. Kim, Y. H. Kim and D. K. Yoon, *RSC Adv.*, 2014, **4**, 26946.

35 D. K. Yoon, J. Yoon, Y. H. Kim, M. C. Choi, J. Kim, O. Sakata, S. Kimura, M. W. Kim, I. I. Smalyukh, N. A. Clark, M. Ree and H.-T. Jung, *Phys. Rev. E: Stat., Nonlinear, Soft Matter Phys.*, 2010, **82**, 041705.

36 I. I. Smalyukh, S. V. Shiyanovskii and O. D. Lavrentovich, *Chem. Phys. Lett.*, 2001, **336**, 88.

37 O. P. Pishnyak, Y. A. Nastishin and O. D. Lavrentovich, *Phys. Rev. Lett.*, 2004, **93**, 041705.

38 T. Ohzono and J. Fukuda, *Soft Matter*, 2012, **8**, 11552.

39 Y. A. Nastishin, C. Meyer and M. Kleman, *Liq. Cryst.*, 2008, **35**, 609.